Title
Integrated IVUS-OCT Imaging for Atherosclerotic Plaque Characterization.

Journal
IEEE Journal of Selected Topics in Quantum Electronics, 20(2)

ISSN
1077-260X

Authors
Li, Xiang
Li, Jiawen
Jing, Joe
et al.

Publication Date
2014-03-01

DOI
10.1109/JSTQE.2013.2274724

Peer reviewed

Published in final edited form as:
IEEE J Sel Top Quantum Electron. 2014 ; 20(2): 7100108–. doi:10.1109/JSTQE.2013.2274724.

Integrated IVUS-OCT Imaging for Atherosclerotic Plaque Characterization

Xiang Li [Member, IEEE],
NIH Ultrasonic Transducer Resource Center and the Department of Biomedical Engineering, University of Southern California, Los Angeles, CA, USA

Jiawen Li,
Department of Biomedical Engineering, the Edwards Life Sciences Center for Advanced Cardiovascular Technology, and Beckman Laser Institute, University of California, Irvine, CA 92697 USA

Joe Jing,
Department of Biomedical Engineering and Beckman Laser Institute, University of California, Irvine, CA 92697 USA

Teng Ma,
NIH Ultrasonic Transducer Resource Center and the Department of Biomedical Engineering, University of Southern California, Los Angeles, CA, USA

Shanshan Liang,
Department of Biomedical Engineering and Beckman Laser Institute, University of California, Irvine, CA 92697 USA

Jun Zhang,
Department of Biomedical Engineering and Beckman Laser Institute, University of California, Irvine, CA 92697 USA

Dilbahar Mohar,
Division of Cardiology, Irvine Medical Center, University of California, Orange, CA 92868 USA

Aidan Raney,
Division of Cardiology, Irvine Medical Center, University of California, Orange, CA 92868 USA

Sari Mahon,
Beckman Laser Institute, University of California, Irvine, CA 92697 USA

Matthew Brenner,
Division of Pulmonary and Critical Care, Irvine Medical Center, University of California, Orange, CA 92868 USA

Pranav Patel,

X. Li and J. Li have equal contributions and are treated as cofirst authors.

Color versions of one or more of the figures in this paper are available online at http://ieeexplore.ieee.org.

Edwards Life Sciences Center for Advanced Cardiovascular Technology, University of California, Irvine, CA 92697 USA

K. Kirk Shung [Life Fellow, IEEE],
NIH Ultrasonic Transducer Resource Center and the Department of Biomedical Engineering, University of Southern California, Los Angeles, CA, USA

Qifa Zhou [Senior Member, IEEE], and
NIH Ultrasonic Transducer Resource Center and the Department of Biomedical Engineering, University of Southern California, Los Angeles, CA, USA

Zhongping Chen
Department of Biomedical Engineering, the Edwards Life Sciences Center for Advanced Cardiovascular Technology, and Beckman Laser Institute, University of California, Irvine, CA 92697 USA

Xiang Li: xiangli@usc.edu; Jiawen Li: jiawenl8810@gmail.com; Joe Jing: jcjing@gmail.com; Teng Ma: tengma@usc.edu; Shanshan Liang: liangshanshan33@gmail.com; Jun Zhang: junzhang@uci.edu; Dilbahar Mohar: dmohar@uci.edu; Aidan Raney: araney@uci.edu; Sari Mahon: mahonsb@uci.edu; Matthew Brenner: mbrenner@uci.edu; Pranav Patel: pranavp@uci.edu; K. Kirk Shung: kkshung@usc.edu; Qifa Zhou: qifazhou@usc.edu; Zhongping Chen: z2chen@uci.edu

Abstract

For the diagnosis of atherosclerosis, biomedical imaging techniques such as intravascular ultrasound (IVUS) and optical coherence tomography (OCT) have been developed. The combined use of IVUS and OCT is hypothesized to remarkably increase diagnostic accuracy of vulnerable plaques. We have developed an integrated IVUS-OCT imaging apparatus, which includes the integrated catheter, motor drive unit, and imaging system. The dual-function imaging catheter has the same diameter of current clinical standard. The imaging system is capable for simultaneous IVUS and OCT imaging in real time. *Ex vivo* and *in vivo* experiments on rabbits with atherosclerosis were conducted to demonstrate the feasibility and superiority of the integrated intravascular imaging modality.

Keywords

IVUS; OCT; intravascular; multimodal

I. Introduction

ATHEROSCLEROSIS is a systemic disease process in which fatty deposits, inflammation, cells, and scar tissue build up within the wall of arteries. The specific disease that atherosclerotic plaques build up within coronary artery is coronary artery diseases (CAD) or coronary heart diseases, which is responsible for the high mortality in the U.S. [1]. Progression of plaques can cause lumen narrowing and intracoronary thrombosis, leading to serious diseases, including heart attack, stroke, and even death. It has been shown that the rupture of vulnerable plaque, which is composed of a thin fibrous cap and underlying necrotic core, is the major cause of luminal thrombosis in acute coronary syndromes [2]–[4].

Various catheter-based intravascular imaging techniques have been investigated to characterize the vessel wall, as well as stent implantation. The conventional intravascular

ultrasound (IVUS) imaging, working in the range of 20–45 MHz, is the most commonly used modality for diagnosing CAD. IVUS possesses the unique property of imaging through luminal blood with large penetration (>5 mm) into vessel wall, which facilitates the evaluation of lumen size, vessel remodeling, and plaque morphology [5], [6]. However, its moderate image contrast and resolution may be insufficient to distinguish the complex constituents in vulnerable plaques [7]–[9]. While the acoustic method has been adopted for clinical use over many years, a number of optical imaging modalities are evolving to provide new insights into the microstructural, compositional, and biochemical features of coronary lesions. The optical modalities for intravascular applications include angioscopy, optical coherence tomography (OCT), laser speckle imaging, near-infrared spectroscopy (NIRS), Raman spectroscopy, and fluorescence imaging, etc. [10]. Among them, intravascular OCT is being extensively investigated in both laboratory and clinical researches. OCT is analogous to IVUS except that infrared light is used instead of ultrasonic waves [11], [12]. OCT allows for a superior resolution (~10 μm) to detect extremely thin fibrous plaque caps. However, the major limitation of OCT is the shallow penetration depth, which is around 1–2 mm [10].

At present, there is no single intravascular imaging modality defined as “gold-standard” for the assessment of plaque vulnerability. Each method mentioned above has unique features and intrinsic shortcomings; therefore, a synergistic approach combining two or more modalities seems favorable [1]. Several investigators have reported different multimodality imaging by combining OCT and fluorescence [13]–[15], IVUS and fluorescence [16], IVUS and photoacoustic [17]–[20], IVUS and NIRS [21]. The integration of IVUS and OCT, which are the two mostly used modalities in the clinic, has been introduced recently [22]–[26]. The combination of IVUS and OCT offers unique advantages of high resolution to resolve superficial microstructures, large penetration depth to detect large lipid pool inside vessel wall, and quick coregistration of IVUS-OCT images. In prior studies, several different prototype integrated IVUS-OCT probes have been introduced.Yin *et al*. [22] reported a probe with side-by-side arranged IVUS and OCT elements. Yang *et al*. [23] reported a probe by incorporating a mirror to redirect acoustic and light beams. Li *et al*. [24] reported a probe with confocally lunched IVUS and OCT beams. These designs are relatively large (outer diameters (OD) > 2.4 mm) and excluded from intracoronary use since the lumen size of coronary artery is quite limited (2–3 mm). Later, Li *et al.* [25] reported a 1-mm-OD probe inside a 4-Fr (1.3 mm) catheter sheath for characterizing coronary atherosclerosis *ex vivo*. Yin *et al.* [26] reported a 0.69-mm-OD probe which fitted in a 3.6-Fr (1.18 mm) catheter sheath and conducted the first *in vivo* animal study. However, in this probe, the rigid tip was more than 10mmlong; optic fiber and electrical wire were sealed in a rigid steel tube through the whole catheter, which significantly limited the catheter’s length and flexibility. Moreover, the imaging system previously reported had a relatively slow frame rate of 4–5 frames/s (fps), which was limited by the rigid probe and the data processing procedure.

In this paper, we report the improvements and technical details on the integrated IVUS-OCT catheter as well as the imaging system, which is capable of real-time imaging for preclinical studies. We built a 1.6 m flexible probe that could fit in a 3.6-Fr catheter sheath, which is a

standard clinically used sheath (Boston Scientific Corporation, Natick, MA, USA). In the integrated IVUS-OCT imaging catheter, the rigid tip is miniaturized (OD: 0.65 mm, length: 5 mm); optical fiber and electrical wire are sealed in a double wound toque coil. The new design is more reliable and flexible. For the imaging system, in utilizing commercial graphics processing units (GPU), we achieved great improvements in computational speed allowing for simultaneous real-time imaging (20 fps) and raw data saving for both modalities. A custom designed motor drive unit is to serve as an interface between imaging catheter and system, as well as to conduct catheter rotation and pull-back. The capability of the integrated IVUS-OCT catheter and imaging system has been demonstrated through *ex vivo* and *in vivo* imaging of rabbit abdominal aortas with atherosclerotic plaques.

II. Integrated IVUS-OCT Imaging Apparatus

The integrated IVUS-OCT imaging apparatus consists of three major components: integrated IVUS-OCT catheter, motor drive unit, and imaging system. A block diagram illustrating the construction of the apparatus is shown in Fig. 1. The integrated IVUS-OCT catheter is a single disposable catheter which is capable of IVUS and OCT imaging simultaneously. The motor drive unit is the interface between catheter and imaging system, which includes a rotational motor, linear pullback stage, and signal coupling joints. The imaging system is composed of several hardware units as well as custom built software, responsible for controlling transmitting, receiving, and processing IVUS and OCT signals.

The overall imaging performance has been benchmarked. The frame rate of the imaging system is now 20 fps with 500 A-lines per revolution and 8192 sampling points in each A-line. The system is capable of real-time displaying and raw data saving for both IVUS and OCT. Pull-back speed is 0.5–5 mm/s. Resolutions of OCT imaging are 8 and 30 μm in axial and lateral directions, respectively. Resolutions of IVUS imaging are 57 and 275 μm in axial and lateral directions, respectively, with a 40 MHz ultrasonic transducer.

A. Integrated IVUS-OCT Catheter

The integrated IVUS-OCT catheter (see the left portion in Fig. 1) features a sequential arrangement of the IVUS transducer and OCT probe, allowing for synchronized imaging while also minimizing the overall probe size. Photographs of the miniature IVUS-OCT catheter are shown in Fig. 2. Fig. 2(a) shows the tip of the catheter, where locates the IVUS transducer and followed by the OCT probe. Within the OCT probe, a single mode fiber is utilized to deliver laser beams, and a 0.35-mm-OD gradient index (GRIN) lens is used for light focusing, followed by a 0.30-mm-OD cylinder microprism for redirecting the focused light beam into tissue. All the optical components are fixed in a polyimide tube with an OD of 0.41 mm. Image scan radius of the OCT probe is 3 mm. The IVUS transducer has an aperture size of 0.4 mm × 0.4 mm and is made of PMN-PT single crystal which has superior piezoelectric properties for building high sensitivity ultrasonic transducers in a small size. The transducer element is connected to a 46 AWG coaxial electrical wire and properly grounded. The IVUS transducer has a center frequency of 40 MHz with a fractional bandwidth of 52%. Two way insertion loss of the transducer is measured to be 15 dB at the center frequency. The IVUS transducer and the OCT probe are placed sequentially inside a 0.65-mm-OD thin-wall stainless tube with a length of 5 mm. Two small windows are

created on the tube to allow for the light beams and acoustic waves to exit unimpeded. There is a fixed offset between the IVUS transducer and the OCT prism, which is measured to be 2 mm. By realigning the IVUS and OCT image frames at this distance, coregistration of the two images can be achieved. The transducer wire and the OCT fiber are confined in a custom double wound torque coil with 0.64 mm OD and 0.4 mm ID. The flexible torque coil ensures accurate and smooth translation of torque to the distal end over a large distance and through tortuous curves. At the proximal end, the transducer wire and the OCT fiber are connected to an electrical slip ring and an OCT connector, respectively, as shown in Fig. 2(c). The catheter is 1.6 m long, with a rigid tip length of 5 mm and the maximum OD of 0.65 mm, which properly fits in a commercial 3.6 Fr catheter sheath and freely rotated, as shown in Fig. 2(b) and (c). The integrated IVUS-OCT catheter is capable for *ex vivo* and *in vivo* imaging studies.

B. Motor Drive Unit

A custom built motor drive unit (see middle portion in Fig. 1) interfaces the IVUS-OCT catheter and imaging system, as shown in Fig. 3. The unit is used for motion control and signal coupling between the rotational part and the stationary part. A rotational motor is linked through a gear fixture with gear ratio of 2:1 to a fiber optic rotary joint, which connects the integrated catheter via the OCT connector to translate rotational torque. The optic rotary joint and a brushed electrical slip ring are used for OCT and IVUS signal coupling, respectively, to allow the whole probe rotate freely. All these components are fixed to a linear translation stage which functions for imaging pull-back.

C. Integrated IVUS-OCT Imaging System

The integrated IVUS-OCT imaging system (see the right portion in Fig. 1) is responsible for transmitting and receiving IVUS and OCT signals, data acquisition (DAQ), and synchronization. The imaging system is composed of laser source, OCT circuits, ultrasound pulser/receiver (P/R), digitizer, computer, as well as custom built software.

In the IVUS subsystem, a Panametrics PR5900 pulser/receiver (Olympus NDT, Kennewick, WA, USA) is used to drive the transducer for pulse generation and subsequent echo signal detection. 2 μJ pulse energy is used to drive the transducer. 26 dB gain and 10–100 MHz band-pass filter are applied to the received RF signals.

In the swept-source OCT (SS-OCT) subsystem, light from a SS (1310 nm center wavelength; 100 nm FWHM bandwidth; 18 mW output power; 20 kHz scanning rate) is split by an 80/20 1 × 2 coupler, with 80% of the power directed to the IVUS-OCT probe and the remaining 20% to the reference arm. Two circulators are used in both arms to redirect back-scattered and back-reflected light to the two input ports of a 50/50 2 × 2 coupler for balanced detection. The measured sensitivity of the OCT subsystem (excluding catheter) is 110 dB. The OCT catheter including rotary joint has the two way insertion loss of 5–7 dB, which is majorly caused by the coupling loss of probe connector, as well as the internal loss of rotary joint.

The laser source generates 20 kHz trigger signals which drive a function generator to synchronize the digitizer and the pulser/receiver. IVUS and OCT signals are fed into separate channels of the 12 bit digitizer and digitized at a sampling rate of 200 MHz. The sampling clock is provided by an external voltage controlled oscillator (VCO). The reason of choosing 200 MHz sampling rate is multiple. High-frequency broadband IVUS signals (40 MHz) require a certain degree of oversampling to avoid aliasing. However, since OCT signals require full fringe period sampling, higher sampling rate will dramatically increase the amount of data generated at both channels of the digitizer. The 200 MHz sampling rate is chosen to balance the data processing time and IVUS-OCT image quality.

The acquired IVUS and OCT signals are processed, displayed, and saved in real time by custom built software. The framework and control mechanics are completely written in C++ while the entirety of the data processing is implemented in NVIDIA's CUDA software development kit (SDK). Processing of the data occurs on a frame by frame basis, with each frame having 500 (up to 1000) A-lines and 8192 points per A-line. The VCO sampling clock is tuned to provide a 200 MHz clock for both channels of the DAQ board. The data set size (8192) per A-line is chosen to be a power of two to speed up fast Fourier transform (FFT) calculations. The acquired frames are transferred to the onboard memory of a GPU (NVIDIA GTX 580, NVIDIA, Santa Clara, CA, USA) for the respective processing. The OCT data first undergo a resampling calibration [27], either by linear interpolation or spline interpolation, to ensure data points (8192 per A-line) are linear in the K domain, followed by the subsequent FFT and logarithmic scaling. The captured IVUS data meanwhile is digitally filtered with a pass band of 20–60 MHz to help isolate the echo signal followed by a Hilbert transform and logarithmic scaling. Both IVUS and OCT sets of data are then scan-converted and formatted into bitmaps and transferred back to the host for display. The GPU acts as a massively parallel processor, allowing for very fast arithmetic computations on large data sets. FFT performance on 1000 A-lines improved from 421 ms on a single CPU thread to 212 μs using the GPU. Logarithm calculations likewise experienced large scaling improvements from 276 ms on the CPU to 1.05 ms on the GPU. Both linear and spline OCT resampling were implanted with almost negligible differences due to the large oversampling of the data. The overall time to process one pair of IVUS and OCT images from the transfer of data to the GPU until the transfer of the processed bitmaps back into the host's memory is on average 10.5 ms. Overall, the system is capable of handling up to 96 frames (assuming 500 A-lines per frame per modality) of IVUS-OCT images per second, including processing, displaying, and raw data saving. However, due to the limited pulse repetition rates of laser source (20 kHz) and ultrasound pulser/receiver (~15 kHz), our system currently works at an imaging speed of 20 fps.

III. Imaging on Rabbit Model of Atherosclerosis

Ex vivo and *in vivo* experiments have been conducted on rabbit abdominal aorta segments with atherosclerotic plaques. The disease model is developed in New Zealand white rabbits. The rabbits were undergone deendothelialization surgical procedures and fed by high-cholesterol diets (0.5% cholesterol and 6% peanut oil) for 12–16 weeks to induce atherosclerotic plaques.

During *ex vivo* imaging, abdominal aortas were harvested freshly and cut into 20-mm-long segments. The imaging catheter was placed through one specimen segment without a guide wire and lying inside a dish filled with saline. The specimen was supported by the catheter and immersed in saline. Attention was paid so the aorta did not touch dish wall to avoid imaging artifacts. The integrated IVUS-OCT probe was spinning inside the catheter sheath. Saline was filled in the sheath for coupling acoustic waves. The whole segment of aorta was imaged by doing pull-back at the speed of 0.5 mm/s. Both IVUS and OCT images were displayed simultaneously while pull-back. If any interested cross section was observed, pull-back can be stopped at that location and OCT catheter can be switched to a visible aiming beam to pinpoint the location on the aorta segment. After imaging, the aorta was fixed in formalin and pinpointed cross sections were stained for histology examination.

Fig. 4 shows IVUS and OCT images acquired at one cross section of rabbit aorta with atherosclerosis. The H&E histology result, shown in Fig. 4(d), indicates an eccentric plaque with intimal thickening around the lumen. The OCT image, shown in Fig. 4(a), displays signal rich at surface and gradually diffused inside the plaque at the position of 7–12 O'clock, which correlates with the dramatically thickened intima in Fig. 4(d). Still in the histology image of Fig. 4(d), a thin elastin layer is observed overlying on the surface of thickened intima at the position of 4–5 O'clock, as indicated by a black arrow in the magnified image (Verhoeff Elastic Stain). This feature is identified as a bright thin layer in OCT image, as indicated by a yellow arrow in Fig. 4(a), owing to OCT's superior resolution for characterizing superficial microstructure. By magnifying this region, OCT displays the intima at higher clarity. On the other hand, the IVUS image, shown in Fig. 4(b), does not identify this ultrathin layer due to insufficient resolution, but IVUS signal penetrates the entire arterial wall and differentiates the intima layer from media layer. Fig. 4(c) shows a fused IVUS and OCT image, from which the intima layer is highlighted by OCT while the entire arterial wall is visible from IVUS. Overall, the OCT image precisely correlates with histological section in the distribution of intimal thickening, although media layer is not seen by OCT due to the lack of depth penetration. The IVUS image shows the media layer clearly defining the outer border of the thickened intima due to higher penetration, although the spatial resolution of the intimal structures is inferior.

In vivo studies have also been successfully conducted on the rabbits with atherosclerosis. The rabbits were anesthetized and went through an open chest surgery. During the surgery, a guide wire was first inserted into the abdominal aorta through an open cut on the thoracic aorta. The guide wire served as a rail to position a 6-Fr access sheath into thoracic aorta. After the access sheath was tied up onto the aorta, the guide wire was pulled out. IVUS-OCT imaging catheter was then inserted through the access sheath down to abdominal aorta. Both IVUS and OCT imaging display was kept on once the catheter was inserted into the access sheath. The imaging catheter has markers on it to record the length inside aorta. During imaging, once an interested cross section was observed on screen, the length of catheter inside aorta was logged. After experiment was done and the rabbit was sacrificed, the catheter was repositioned to the interested cross sections and OCT probe was switched to a visible aiming beam to pinpoint the location for histology. OCT images were displayed before pinpointing to ensure the correct cross section was located.

Fig. 5 shows the OCT and IVUS images acquired before and after flushing, as well as the corresponding H&E histology image. Since the blood is highly scattering for light instead of ultrasound, the aorta structures can only be identified by IVUS without flushing, as shown in Fig. 5(a) and (b). Blood clearance flushing was performed with 10 mL Omnipaque coronary angiography contrast (iohexol, 350 mI/mL) at ~3 mL/s. After the infusion of flushing agent, OCT displayed a clear view of the aorta, as shown in Fig. 5(c). As the flushing diluted and replaced the blood temporarily, IVUS also obtained a clearer view of the lumen border, as shown in Fig. 5(d). In the IVUS image, there is a dark band inside vessel wall, which is an indication of lipid rich region (Lip). This feature is consistent with the lipid rich plaque (foam cells) identified in the histology image, as shown in Fig. 5(f). On the other hand, in the OCT image, signal is rapidly attenuated behind the lumen border, which indicates the existence of lipid rich plaque. However, the shallow penetration of OCT is insufficient to see through the entire depth of lipid region.

Throughout the imaging experiments, IVUS demonstrates the capability to see through blood and the deep penetration to evaluate the whole depth of plaques. On the other hand, OCT demonstrates ultrafine resolution to define the superficial microstructures, which is critical for diagnosing the vulnerability of plaques. The synergy of the combination of IVUS and OCT brings the unique merits of each modality into one catheter, which not only provides complementary information from the two modalities but also reduces the fabrication costs and operational risks, compared to using the two modalities separately.

IV. Discussion and Conclusion

We have successfully developed an integrated IVUS-OCT imaging apparatus for intracoronary imaging diagnosis. The miniature integrated IVUS-OCT catheter has the same OD as current clinical standard. The catheter is functional for simultaneously IVUS and OCT imaging in real time. The motor drive unit facilitates the interfacing between the catheter and imaging system, which also provides convenience for operation. The imaging system has achieved the frame rate of 20 fps for both IVUS and OCT for real-time displaying and raw data saving. Imaging pullback speed is 0.5–5 mm/s. The functionality of the entire apparatus has been validated through *ex vivo* and *in vivo* imaging of rabbit aorta with atherosclerosis.

Though the testing results are promising for the integrated catheter technology, there are still several technical aspects need to be improved before this dual-modality imaging can be applied to the clinic.

The rigid tip of the integrated catheter is 5 mm in length currently (2 mm in commercial IVUS catheter), which might cause difficulty for the catheter to pass through some significantly tortured strictures, as well as nonuniform rotational distortion (NURD) artifacts in the image. The length of the rigid tip is mainly limited by the multiple optical components in an OCT probe, such as GRIN lens and prism. In the future, we plan to replace the OCT probe by a ball-lens-based design, which could reduce the tip length to 2–3 mm. The coplanar designs [22], [25] may also help to reduce the rigid length, but at the cost of widening OD, which is even more undesirable. However, the coplanar designs have the

unique advantage of imaging at the same cross section simultaneously, which implies the coregistration of IVUS and OCT is unaffected by the cardiac cycles. For the design of sequentially arranged IVUS and OCT in this report, the offset distance between IVUS and OCT is 2 mm and can be reduced by 50% or more if a ball-lens-based OCT probe is used. Reducing the offset distance is desired for synchronizing IVUS and OCT images, as well as shortening the rigid tip of catheter.

Imaging frame rate of the integrated modality needs to be improved. The imaging speed affects the amount of flushing agent needed to create the time window of blood clearance, which are directly related to the operation safety. The state-of-the-art OCT catheter can achieve 100 fps with 500 A-lines per frame. Our system currently can work at 20 fps with 500 A-lines per frame. The major limiting factor is the repetition rate of ultrasound pulse generator (~15 kHz) and swept laser source (20 kHz). In order to achieve the speed of the state-of-the-art OCT, the repetition rate needs to reach up to 50 kHz or higher for both subsystems. At such speed, each IVUS A-line can still image with 7.5mmradius and allow another 10 μs for ultrasound echo to die out before firing next IVUS pulse. Another frame rate limiting factor may be the brushed electrical slip ring, which needs direct contact between stationary and rotation conductors. Alternatives can be a rotary transformer or capacitive coupler. The ideal solution for signal coupling is to have an integrated noncontact rotary coupler for both electrical and optical signals.

In conclusion, we reported an integrated IVUS-OCT imaging apparatus, as well as results obtained from *ex vivo* and *in vivo* tests. The results of experiments well demonstrated its capability for small animal studies, providing high resolution and high penetration depth for a better assessment of vulnerable plaques. After solving some potential technical issues, this integrated modality is promising for using in clinical studies.

Acknowledgments

The authors would like to thank T. Burney, D. Mukai, D. Yoon and E. Steward for their assistance during the surgical procedure. We also acknowledge L. Liaw and L. Li for their assistance in histology. Institutional support from the Beckman Laser Institute Endowment is also gratefully acknowledged. Dr. Z. Chen has a financial interest in OCT Medical Imaging Inc., which, however, did not support this work. Please address all correspondence to Dr. Q. Zhou and Dr. Z. Chen.

This work was supported in part by the NIH under Grants R01EB10090, R01CA124967, K25HL102005, P41EB015890, and P41-EB2182.

References

1. Puri R, Worthley MI, Nicholls SJ. Intravascular imaging of vulnerable coronary plaque: Current and future concepts. Nature Rev. Cardiol. 2011; 8(no. 3):131–139. [PubMed: 21263456]
2. Davies MJ, Thomas A. Thrombosis and acute coronary-artery lesions in sudden cardiac ischemic death. N. Engl. J. Med. 1984; 310(no. 18):1137–1140. [PubMed: 6709008]
3. Virmani R, Kolodgie FD, Burke AP, Farb A, Schwartz SM. Lessons from sudden coronary death: A comprehensive morphological classification scheme for atherosclerotic lesions. Arterioscler. Thromb. Vasc. Bio. 2000; 20(no. 5):1262–1275. [PubMed: 10807742]
4. Virmani R, Kolodgie FD, Burke AP, Finn AV, Gold HK, Tulenko TN, Wrenn SP, Narula J. Atherosclerotic plaque progression and vulnerability to rupture. Arterioscler. Thromb. Vasc. Biol. 2005; 25(no. 10):2054–2061. [PubMed: 16037567]

5. Nissen SE, Gurley JC, Grines CL, Booth DC, McClure R, Berk M, Fischer C, DeMaria AN. Intravascular ultrasound assessment of lumen size and wall morphology in normal subjects and patients with coronary artery disease. Circulation. 1991; 84(no. 3):1087–1099. [PubMed: 1884441]
6. Nicholls SJ, Stephen J, Tuzcu EM, Sipahi I, Schoenhagen P, Nissen SE. Intravascular ultrasound in cardiovascular medicine. Circulation. 2006; 114(no. 4):e55–e59. [PubMed: 16864731]
7. Pasterkamp G, Falk E, Woutman H, Borst C. Techniques characterizing the coronary atherosclerotic plaque: Influence on clinical decision making. J. Amer. College Cardiol. 2000; 36(no. 1):13–21.
8. Foster FS, Pavlin CJ, Harasiewicz KA, Christopher DA, Turnbull DH. Advances in ultrasound biomicroscopy. Ultrasound Med. Biol. 2000; 26(no. 1):1–27. [PubMed: 10687788]
9. Sawada T, Shite J, Garcia-Garcia HM, Shinke T, Watanabe S, Otake H, Matsumoto D, Tanino Y, Ogasawara D, Kawamori H, Kato H, Miyoshi N, Yokoyama M, Serruys PW, Hirata K. Feasibility of combined use of intravascular ultrasound radiofrequency data analysis and optical coherence tomography for detecting thin-cap fibroatheroma. Eur. Heart J. 2008; 29(no. 9):1136–1146. [PubMed: 18397871]
10. Suter MJ, Nadkarni SK, Weisz G, Tanaka A, Jaffer FA, Bouma BE, Tearney GJ. Intravascular optical imaging technology for investigating the coronary artery. JACC: Cardiovascular Imaging. 2011; 4(no. 9):1022–1039. [PubMed: 21920342]
11. Patwari P, Weissman NJ, Boppart SA, Jesser C, Stamper D, Fujimoto JG, Brezinski ME. Assessment of coronary plaque with optical coherence tomography and high-frequency ultrasound. Amer. J. Cardiol. 2000; 85(no. 5):641–644. [PubMed: 11078281]
12. Huang D, Swanson EA, Lin CP, Schuman JS, Stinson WG, Chang W, Hee MR, Flotte T, Gregory K, Puliafito CA. Optical coherence tomography. Science. 1991; 254(no. 5035):1178–1181. [PubMed: 1957169]
13. Yoo H, Kim JW, Shishkov M, Namati E, Morse T, Shubochkin R, McCarthy JR, Ntziachristos V, Bouma BE, Jaffer FA, Tearney GJ. Intra-arterial catheter for simultaneous microstructural and molecular imaging *in vivo*. Nature Med. 2011; 17(no. 12):1680–1684. [PubMed: 22057345]
14. Liang S, Saidi A, Jing J, Liu G, Li J, Zhang J, Sun C, Narula J, Chen Z. Intravascular atherosclerotic imaging with combined fluorescence and optical coherence tomography probe based on a double-clad fiber combiner. J. Biomed. Opt. 2012; 17(no. 7):070501-1–070501-3. [PubMed: 22894457]
15. Mavadia J, Xi J, Chen Y, Li X. An all-fiber-optic endoscopy platform for simultaneous OCT and fluorescence imaging. Biomed. Opt. Exp. 2012; 3(no. 11):2851–2859.
16. Bec J, Xie H, Yankelevich DR, Zhou F, Sun Y, Ghata N, Aldredge R, Marcu L. Design, construction, and validation of a rotary multifunctional intravascular diagnostic catheter combining multispectral fluorescence lifetime imaging and intravascular ultrasound. J. Biomed. Opt. 2012; 17(no. 10):106012-1–106012-10. [PubMed: 23224011]
17. Wang B, Su JL, Karpiouk AB, Sokolov KV, Smalling RW, Emelianov SY. Intravascular photoacoustic imaging. IEEE J. Quantum, Electron. 2010; 16(no. 3):588–599. [PubMed: 21359138]
18. Jansen K, van der Steen AF, van Beusekom HM, Oosterhuis JW, van Soest G. Intravascular photoacoustic imaging of human coronary atherosclerosis. Opt. Lett. 2011; 36(no. 5):597–599. [PubMed: 21368919]
19. Wei W, Li X, Zhou Q, Shung KK, Chen Z. Integrated ultrasound and photoacoustic probe for co-registered intravascular imaging. J. Biomed. Opt. 2011; 16(no. 10):106001-1–106001-6. [PubMed: 22029348]
20. Li X, Wei W, Zhou Q, Shung KK, Chen Z. Intravascular photoacoustic imaging at 35 and 80 MHz. J. Biomed. Opt. 2012; 17(no. 10):106005-1–106005-6. [PubMed: 23224004]
21. Study of near infrared spectroscopy (NIRS) and intravascular ultrasound (IVUS) combination coronary catheter (SAVOIR). 2012 Dec 12. http://clinicaltrials.gov/ct2/show/NCT00901446
22. Yin J, Yang HC, Li X, Zhang J, Zhou Q, Hu C, Shung KK, Chen Z. Integrated intravascular optical coherence tomography ultrasound imaging system. J. Biomed. Opt. 2010; 15(no. 1): 010512-1–010512-3. [PubMed: 20210424]
23. Yang HC, Yin J, Hu C, Cannata J, Zhou Q, Zhang J, Chen Z, Shung KK. A dual-modality probe utilizing intravascular ultrasound and optical coherence tomography for intravascular imaging

applications. IEEE Trans. Ultrason. Ferroelectr. Freq. Control. 2010 Dec; 57(no. 12):2839–2843. [PubMed: 21156380]

24. Li X, Yin J, Hu C, Zhou Q, Shung KK, Chen Z. High-resolution coregistered intravascular imaging with integrated ultrasound and optical coherence tomography probe. Appl. Phys. Lett. 2010; 97(no. 13):133702-1–133702-3. [PubMed: 20981274]
25. Li BH, Leung ASO, Soong A, Munding CE, Lee H, Thind AS, Munce NR, Wright GA, Rowsell CH, Yang VXD, Strauss BH, Foster FS, Courtney BK. Hybrid intravascular ultrasound and optical coherence tomography catheter for imaging of coronary atherosclerosis. Catheter. Cardiovasc. Interv. 2013; 8(no. 3):494–507. [PubMed: 22566368]
26. Yin J, Li X, Jing J, Li J, Mukai D, Mahon S, Edris A, Hoang K, Shung KK, Brenner M, Narula J, Zhou Q, Chen Z. Novel combined miniature optical coherence tomography ultrasound probe for in vivo intravascular imaging. J. Biomed. Opt. 2011; 16(no. 6):060505-1–060505-3. [PubMed: 21721799]
27. Yasuno Y, Madjarova VD, Makita S, Akiba M, Morosawa A, Chong C, Sakai T, Chan KP, Itoh M, Yatagai T. Three-dimensional and high-speed swept-source optical coherence tomography for in vivo investigation of human anterior eye segments. Opt. Exp. 2005; 13(no. 26):10652–10664.

Biographies

Xiang Li received the B.E. degree from Zhejiang University, Hangzhou, China, in 2007, the M.S. and Ph.D. degrees from the University of Southern California (USC), Los Angeles, CA, USA, in 2010 and 2012, respectively. He started his Ph.D. study in 2008 under the support of the USC Provost's Fellowship under the direction of Dr. K. K. Shung and Dr. Q. Zhou in the NIH Ultrasonic Transducer Resource Center (UTRC). In 2010, he won the Student Paper Competition Award at the IEEE International Ultrasonics Symposium, San Diego, CA, USA. His research interests include medical ultrasound technology, intravascular ultrasound (IVUS) imaging, integrated IVUS-OCT imaging, and intravascular photoacoustic imaging. He has published 20 peer-reviewed journal papers and 16 conference proceedings. He is currently working at GE Global Research, Niskayuna, NY, USA, since 2012.

Jiawen Li received the bachelor's degree in optical and electrical engineering from Zhejiang University, China, in 2010. During her undergraduate career, she spent 2 years researching on measurement of 3-D velocity vector by Doppler Optical coherence tomography (two papers published). She is currently working toward the Ph.D. degree in the University of California, Irvine (UC Irvine), under the instruction of Dr. Z. Chen. Her research interests include Multimodality intravascular imaging for identification of

vulnerable plaque, Doppler optical coherence tomography imaging, and ultrasmall optical fiber endoscope. Her research has been highlighted in UC Irvine website.

Joe Jing, photograph and biography not available at the time of publication.

Teng Ma, photograph and biography not available at the time of publication.

Shanshan Liang, photograph and biography not available at the time of publication.

Jun Zhang, photograph and biography not available at the time of publication.

Dilbahar Mohar, photograph and biography not available at the time of publication.

AidanRaney, photograph and biography not available at the time of publication.

Sari Mahon, photograph and biography not available at the time of publication.

Matthew Brenner, photograph and biography not available at the time of publication.

Pranav Patel, photograph and biography not available at the time of publication.

K. Kirk Shung received the B.S. degree in electrical engineering from Cheng-Kung University in Taiwan in 1968; the M.S. degree in electrical engineering from the University of Missouri, Columbia, MO, USA, in 1970; and the Ph.D. degree in electrical engineering from the University of Washington, Seattle, WA, USA, in 1975. He taught at The Pennsylvania State University, University Park, PA, USA, for 23 years before moving to the Department of Biomedical Engineering, University of Southern California, Los Angeles, CA, USA, as a Professor in 2002. He has been the Director of the NIH Resource on Medical Ultrasonic Transducer Technology since 1997. Dr. Shung is a Life Fellow of IEEE and a Fellow of the Acoustical Society of America and the American Institute of Ultrasound in Medicine. He is a Founding Fellow of American Institute of Medical and Biological Engineering. He received the IEEE Engineering in Medicine and Biology Society Early Career Award in 1985 and was the coauthor of a paper that received the best paper award for the IEEE Transactions on Ultrasonics, Ferroelectrics, and Frequency Control (UFFC) in 2000. He was elected an outstanding alumnus of Cheng-Kung University in Taiwan in 2001. He was selected as the Distinguished Lecturer for the IEEE UFFC society for 2002– 2003. He received the Holmes Pioneer Award in Basic Science from American Institute of Ultrasound in Medicine in 2010. He was selected to receive the academic career achievement award from the IEEE Engineering in Medicine and Biology Society in 2011. Dr. Shung has published more than 400 papers and book chapters. He is the author of the textbook *Principles of Medical Imaging* (Academic, 1992) and the textbook *Diagnostic*

Ultrasound: Imaging and Blood Flow Measurements, (CRC Press, 2005). He coedited the book *Ultrasonic Scattering by Biological Tissues*, (CRC Press, 1993). He is an Associate Editor of the IEEE TRANSACTIONS ONULTRASONICS, Ferroelectrics, and Frequency Control and a member of the editorial board of *Ultrasound in Medicine and Biology*. His research interests include ultrasonic transducers, high-frequency ultrasonic imaging, ultrasound microbeams, and ultrasonic scattering in tissues.

Qifa Zhou received the Ph.D. degree from Xi'an Jiaotong University, China, in 1993. He is currently a Research Professor at the NIH Resource on Medical Ultrasonic Transducer Technology and the Department of Biomedical Engineering and Industry and System Engineering, University of Southern California (USC), Los Angeles, CA, USA. Before joining USC in 2002, he worked at the Department of Physics, Zhongshan University, China, the Department of Applied Physics, Hong Kong Polytechnic University, and the Materials Research Laboratory, Pennsylvania State University. Dr. Zhou is a Senior Member of IEEE Ultrasonics, Ferroelectrics, and Frequency Control (UFFC) Society and a member of the UFFC Society's Ferroelectric Committee. He is also a member of the Technical Program Committee of the IEEE International Ultrasonics Symposium. He is an Associate Editor of the IEEE Transactions on Ultrasonics, Ferroelectrics, and Frequency Control. His current research interests include the development of ferroelectric thin films, MEMS technology, nanocomposites, modeling, and fabrication of high-frequency ultrasound transducers and arrays for medical imaging applications, such as photoacoustic imaging and intravascular imaging. He has published more than 130 journal papers in this area.

Zhongping Chen received the B.S. degree in applied physics from Shanghai Jiao Tong University, Shanghai, China, in 1982, the M.S. degree in electrical engineering from Cornell University, NY, USA, in 1987, and the Ph.D. degree in applied physics from Cornell University in 1993. He is currently a Professor of biomedical engineering and the Director of F-OCT Laboratory at the University of California, Irvine, CA, USA. He is a cofounder and the Board Chairman of OCT Medical Imaging, Inc. His research interests encompass the areas of biomedical photonics, microfabrication, biomaterials, and biosensors. His research group has pioneered the development of functional optical coherence tomography, which simultaneously provides high-resolution 3-D images of tissue structure, blood flow, and birefringence. He has published more than 180 peer-reviewed papers and review articles and holds a number of patents in the fields of biomaterials, biosensors, and biomedical imaging.

Dr. Chen is a Fellow of the American Institute of Medical and Biological Engineering (AIMBE), a Fellow of SPIE, and a Fellow of the Optical Society of America.

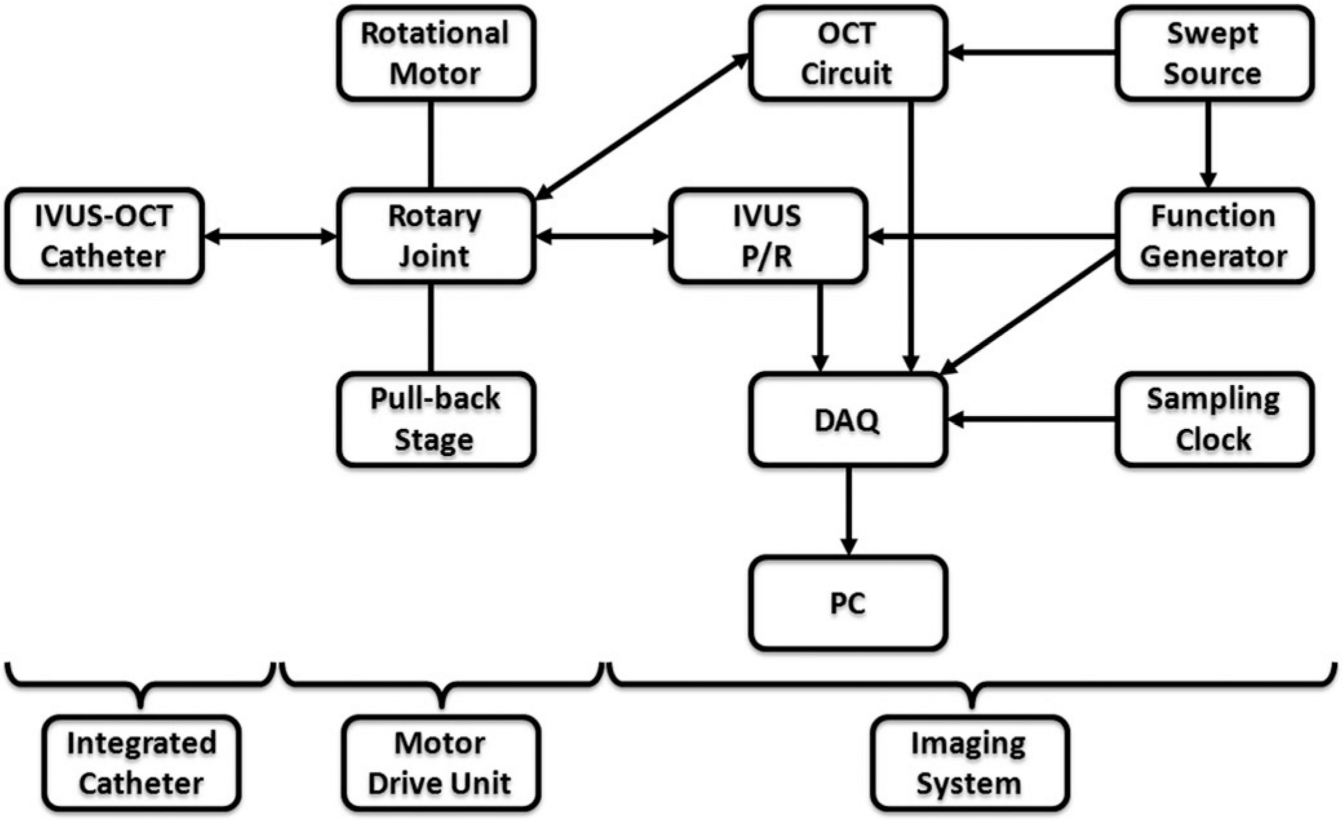

Fig. 1.

Diagram of the integrated IVUS-OCT imaging apparatus, which is composed of integrated IVUS-OCT catheter; motor drive unit and imaging system.

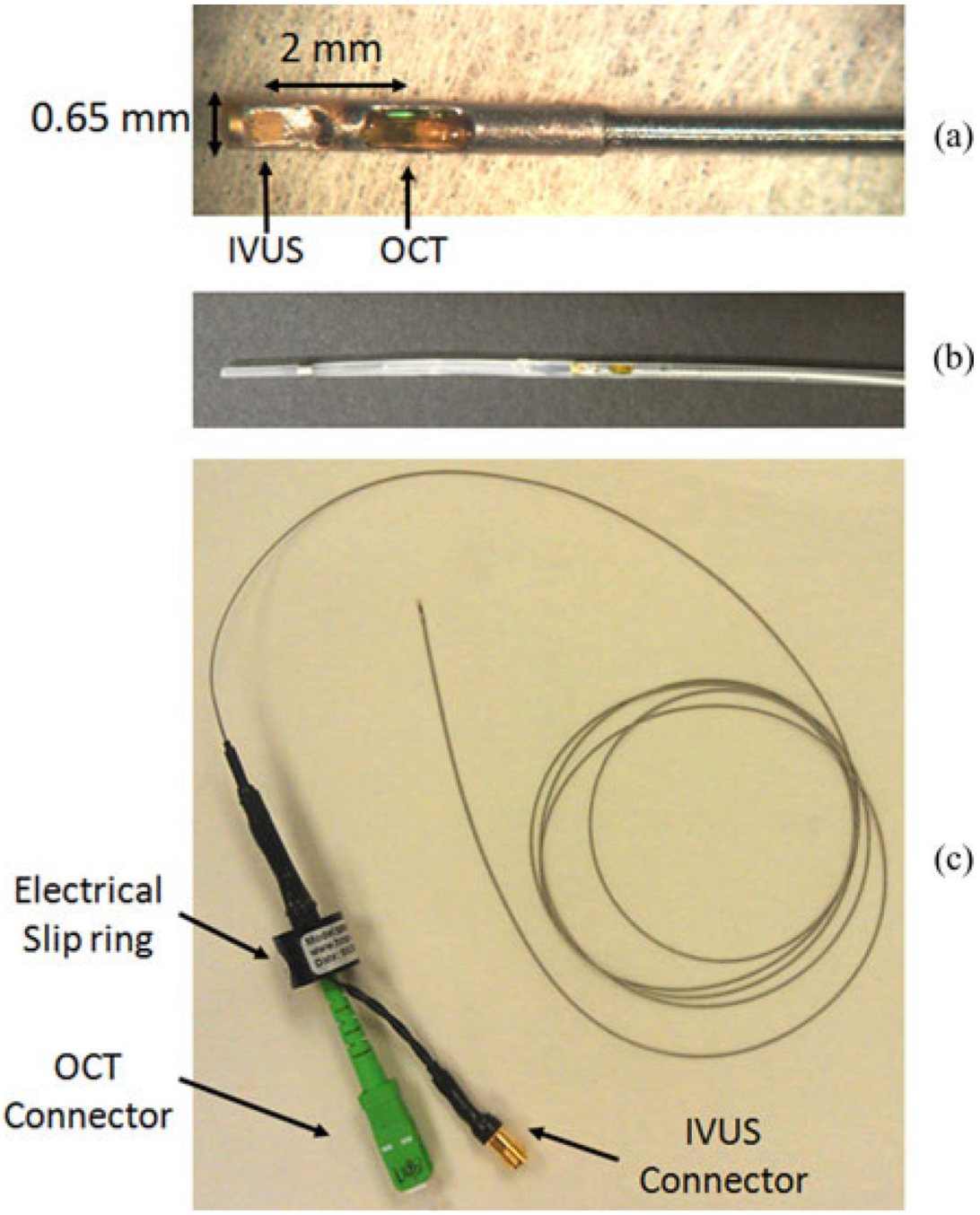

Fig. 2.

(a) The distal end of the miniature integrated IVUS-OCT probe, which is composed of IVUS transducer and OCT probe; (b) The integrated IVUS-OCT probe fits in a clinical standard 3.6 Fr catheter sheath; A bird-view of the whole catheter.

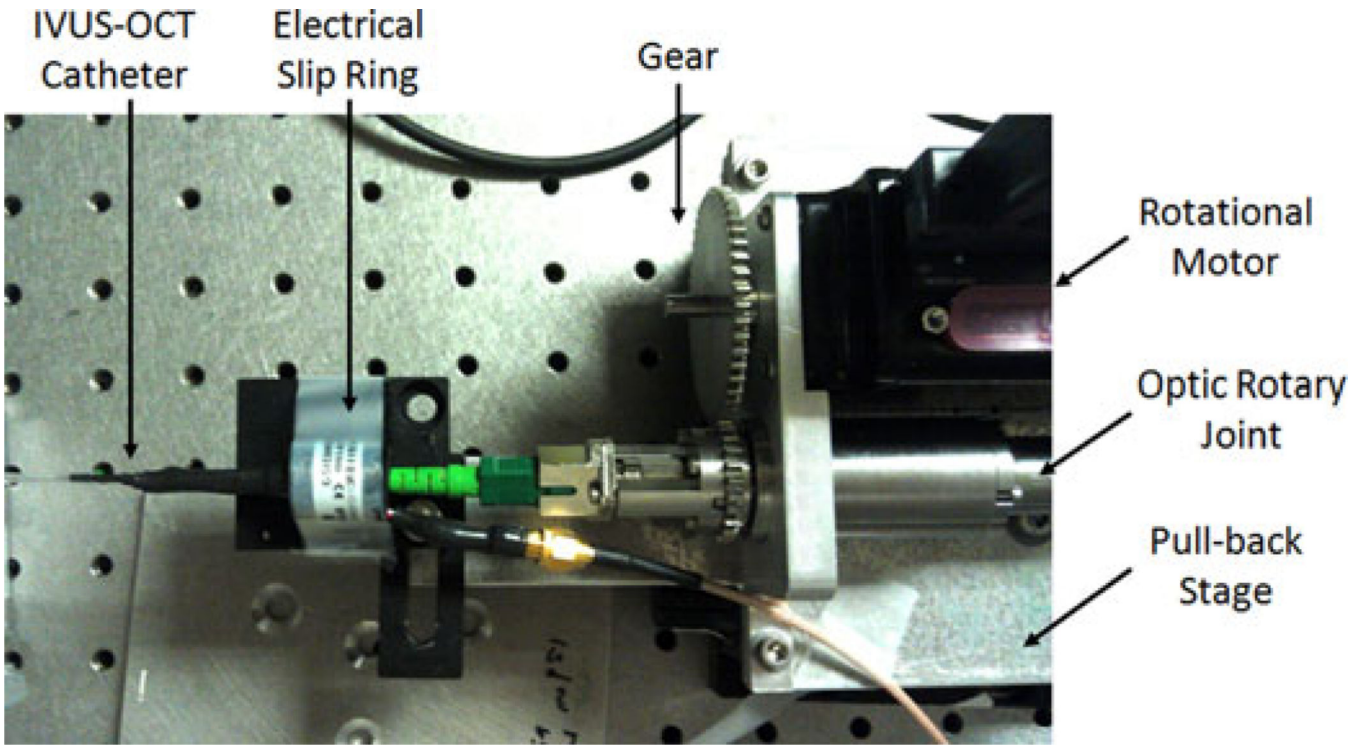

Fig. 3.

A rotary joint device connects the rotational and pull-back motor; and couples electrical and optical signals between the rotational and stationary parts.

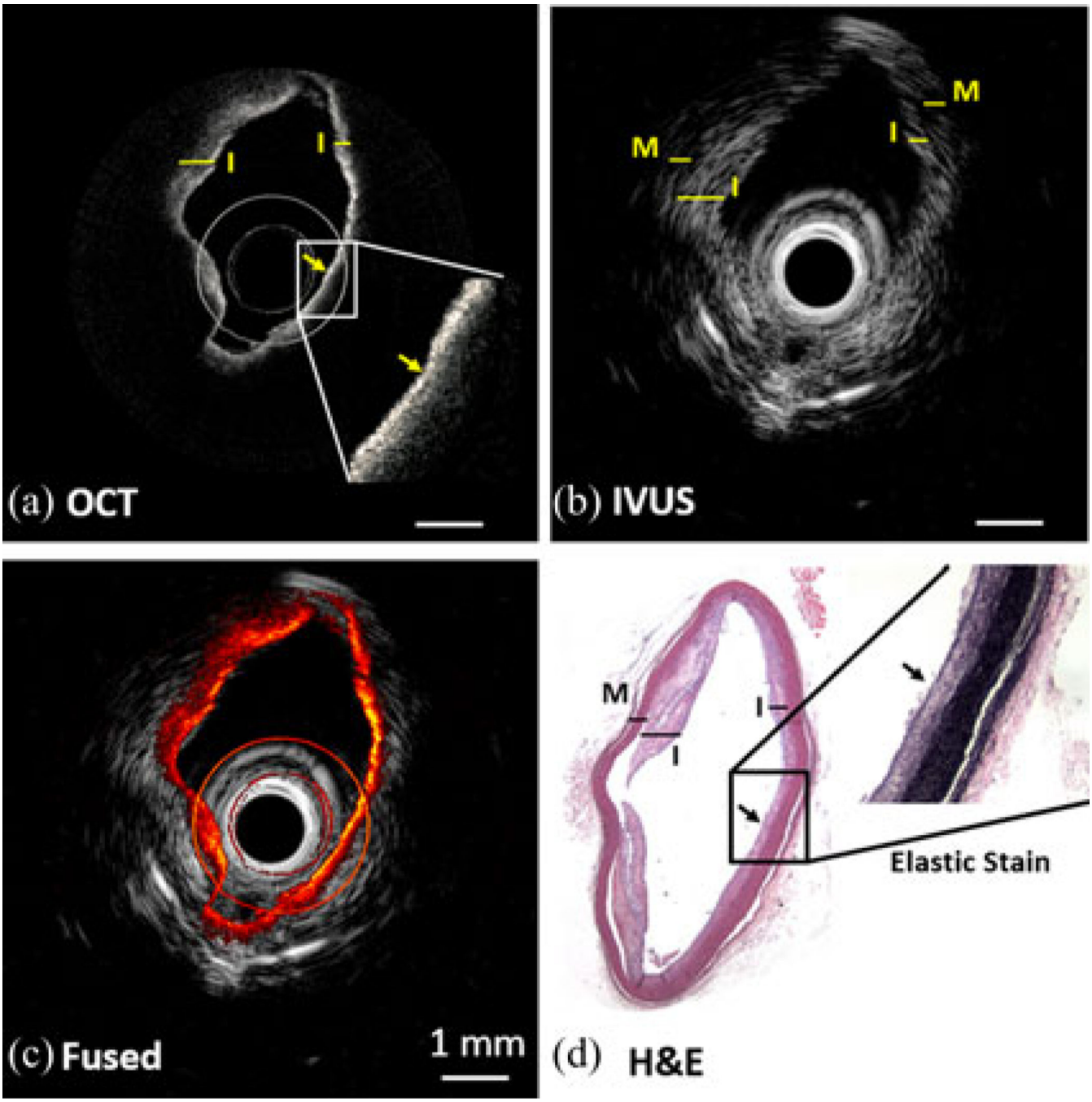

Fig. 4.

Ex vivo OCT (a) IVUS (b) fused IVUS-OCT image (c) and corresponding H&E histology (d) images of an atherosclerotic rabbit aorta with eccentric plaque. The magnified histology in (d) is Verhoff elastic stain which highlights elastin fibers. I: intima; M: media. The yellow and black arrows point to an elastin layer in OCT and histology images, respectively.

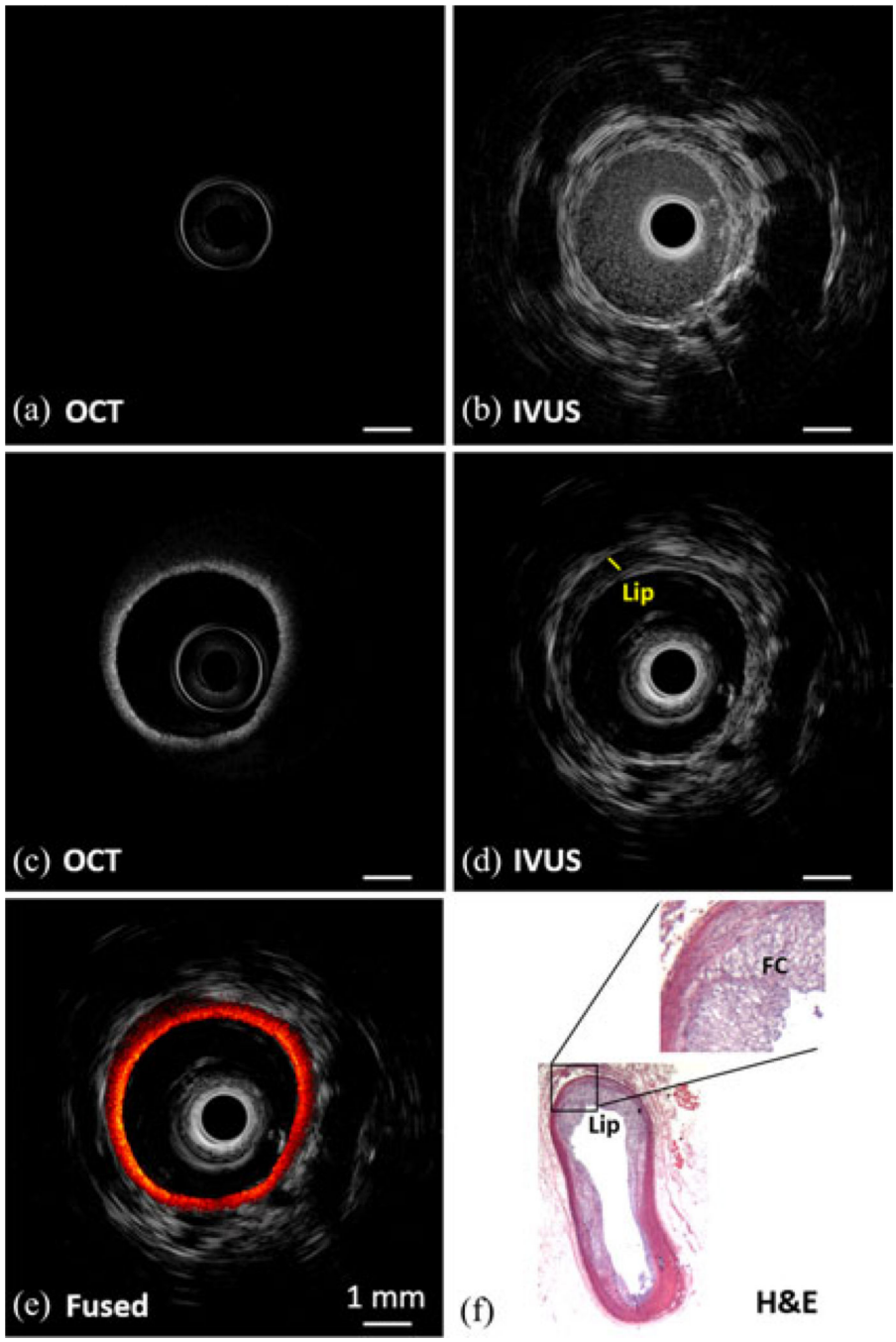

Fig. 5.

OCT (a) and IVUS (b) images of a rabbit abdominal aorta obtained *in vivo* without flushing; OCT (c) and IVUS (d) images obtained after flushing; fused image (e) of OCT (c) and IVUS (d); and corresponding H&E histology image (f). Lip: lipid rich plaque; FC: foam cell.